

## Pick-and-Place Using Chemically Actuated Microgrippers

Jatinder S. Randhawa,<sup>†</sup> Timothy G. Leong,<sup>†</sup> Noy Bassik,<sup>§,†</sup> Bryan R. Benson,<sup>†</sup>  
Matthew T. Jochmans,<sup>||</sup> and David H. Gracias<sup>‡,\*,†</sup>

Department of Chemical and Biomolecular Engineering, Johns Hopkins University, Baltimore, Maryland 21218

Received September 8, 2008; E-mail: dgracias@jhu.edu

In this communication, we demonstrate the concept of single-use, chemically triggered, reversible tools in the form of mobile grippers that can be used to manipulate micro-objects. Both the closing and opening of the mobile grippers are triggered by chemicals, namely acetic acid ( $\text{CH}_3\text{COOH}$ ) and hydrogen peroxide ( $\text{H}_2\text{O}_2$ ), respectively. The grippers close and open en masse based on chemical etching, which results in mechanical property changes within trilayer joints patterned within the gripper, and no external power is needed for operation. We describe the actuation of the gripper using a multilayer thin film model and demonstrate utility of the gripper by picking-and-placing  $200\ \mu\text{m}$  diameter tubes and beads. Our pick-and-place microgripper is a step toward the development of functional Micro Chemo-Mechanical Systems (MCMS), which are actuated by chemistry as opposed to electricity [as in Micro Electro-Mechanical Systems (MEMS)].

A dominant paradigm in engineering is to fabricate microsystems that are triggered by electrical, thermal, or pneumatic signals.<sup>1</sup> While actuation by these signals has achieved a high degree of control and precision in certain applications, several limitations exist. Electrically actuated devices, for example, typically need wiring, thereby limiting the miniaturization, maneuverability, and the ability to trigger many devices simultaneously when they are spatially separated. In contrast, biological machinery widely utilizes chemically actuated triggers which enable autonomous function and high selectivity. A classic example is the antibody–antigen binding that triggers macrophage function.<sup>2</sup> As compared to electrical feedback loops, coupled chemical reactions can enable a high degree of autonomous function as well as multistep behavior.<sup>3</sup>

We fabricated three-dimensional (3D) microgrippers in a highly parallel and cost-effective manner using two layers of conventional photolithography.<sup>4</sup> The grippers were shaped like hands and have a gold (Au, 500 nm thick) coated nickel (Ni, 6  $\mu\text{m}$  thick) palm and phalanges separated by trilayer joints. The smallest grippers had a dimension of  $700\ \mu\text{m}$  when open and  $\sim 200\ \mu\text{m}$  when closed. Since Ni is ferromagnetic, the grippers could be moved with a magnet from distances as far away as several centimeters. The Au coating improved the etch selectivity of the underlying Ni layer. The trilayer joints were composed of films of the following thickness; 50 nm chromium (Cr), 250 nm copper (Cu), and 3.5  $\mu\text{m}$  of a commercial novolac photopatternable polymeric resin (Figure 1a, and details in the Supporting Information). The grippers were released from the Si substrate on which they were fabricated by dissolving a water soluble polyvinyl alcohol (PVA) sacrificial layer.

The operation of the gripper was controlled by a Cr/Cu metallic bilayer with another layer of polymer acting as the trigger (Figure 1). Stressed bilayers have been seen to release residual stress by

bending spontaneously upon release from substrates.<sup>5</sup> However, in our case the grippers remained flat when released from the substrate, since the stiff polymer prevented the spontaneous bending of the stressed bilayer within the joints (Figure 1a–c). When  $\text{CH}_3\text{COOH}$  was added to the water, the polymer dissolved<sup>6</sup> causing the joints to bend and the grippers to close (Figure 1d–f). The gripper then remained closed and could be moved around without reopening. Subsequently, when  $\text{H}_2\text{O}_2$  was added to the aqueous acetic acid solution (1–5% w/w), the Cu layer dissolved,<sup>7</sup> causing the Cr joint to straighten out and the gripper to reopen (Figure 1g–i).

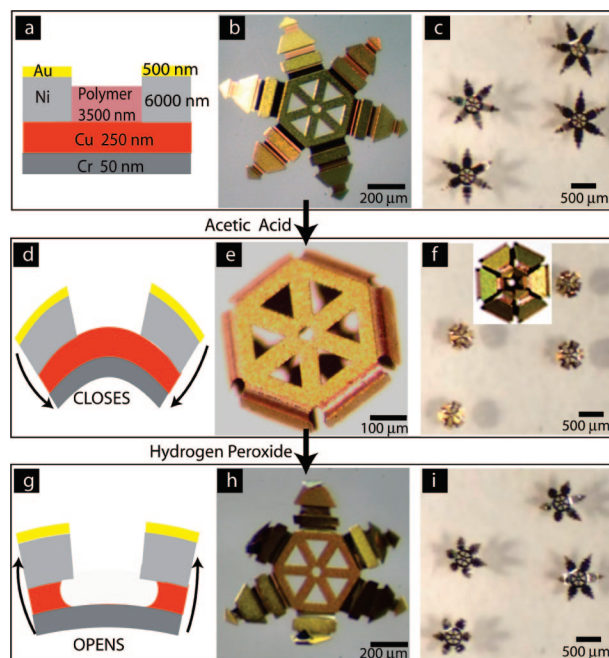


**Figure 1.** (a) Schematic diagram of the trilayer hinge joint between two Au coated Ni phalanges. Optical microscopy image of (b) a single microgripper and (c) many microgrippers in water. (d) Schematic diagram of the microgripper closing when acetic acid dissolves the polymer layer within the hinge. Optical microscopy image of (e) a single microgripper and (f) many microgrippers closing upon addition of acetic acid (inset shows the view from the bottom of a closed microgripper). (g) Schematic diagram of the microgripper opening when  $\text{H}_2\text{O}_2$  dissolves the Cu layer within the hinge. Optical microscopy image of (h) a single microgripper and (i) many microgrippers opening upon addition of  $\text{H}_2\text{O}_2$ .

To understand the mechanical response of the joints, we modeled the trilayer joint using a multilayer thin film model<sup>8</sup> (Figure 2, details in the Supporting Information). When the polymer is present, the joints remain almost flat (Figure 2 a,b; state A), which agrees with the small hinge angle ( $4^\circ$ ) predicted by the model (Figure 2c, state A). When the polymer is dissolved, the grippers close (Figure 2 a, b; state B); the model predicts a hinge angle of  $\sim 68^\circ$  after

<sup>§</sup> School of Medicine, Johns Hopkins University, Baltimore, MD.

<sup>||</sup> Towson High School, Baltimore, MD.

<sup>‡</sup> Department of Chemistry, Johns Hopkins University, Baltimore, MD.

<sup>†</sup> Department of Chemical and Biomolecular Engineering, Johns Hopkins University.

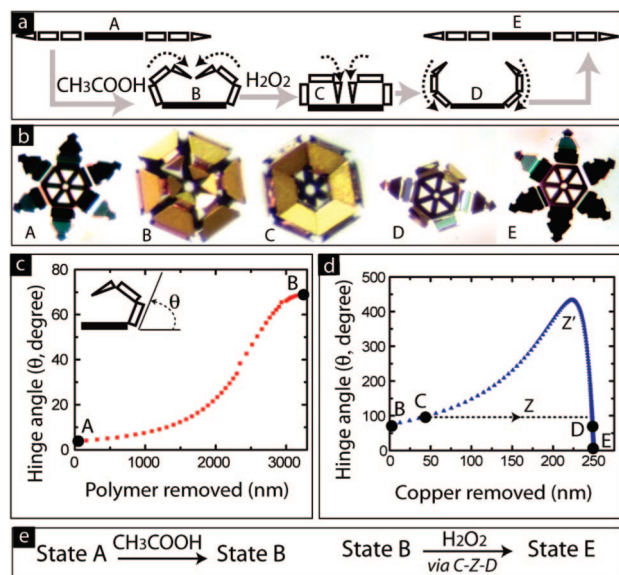


**Figure 2.** (a) Schematic diagram and corresponding (b) optical microscopy images showing the different steps during closing and opening of the gripper. The thin film multilayer model predicts a change in the hinge angle upon (c) removal of the polymer causing the gripper to close and (d) removal of the copper causing the gripper to first tighten and then open. (e) Schematic diagram chemo-mechanical actuation.

complete removal of polymer (Figure 2 c; state B). Hence,  $\text{CH}_3\text{COOH}$  causes the gripper to move from state A to state B (Figure 2e).

The opening mechanism is, however, more complicated. When  $\text{H}_2\text{O}_2$  is added to the aqueous  $\text{CH}_3\text{COOH}$  solution, the Cu starts to dissolve. Initially, we observed that the grippers tighten (Figure 2 a, b; state C); this behavior is validated by the model (Figure 2 d; state C) which actually predicts an increase in hinge angle (path Z', Figure 2d). In an unpatterned film, this large angle is equivalent to bending in multiple turns. However, since the bending of the joints in the gripper is restricted as a consequence of the phalanges pushing into each other, the gripper merely tightens. When the Cu is completely dissolved however, a bare Cr film remains which causes the grippers to open (Figure 2 a,b; state D) and eventually flatten out completely (Figure 2 a,b; state E); this behavior is in agreement with the model (Figure 2 d; state D,E). Hence, the  $\text{H}_2\text{O}_2$  causes the grippers to transition from state B to E, along path Z.

Since the gripper could be both closed and opened by chemicals, it was used to accomplish the pick-and-place function. Pick-and-place<sup>9</sup> is ubiquitous in human engineering, specifically enabling high throughput, assembly line manufacturing. The function involves either automated or operator assisted picking up of an object at one location and placing it at another specified location. Briefly, this engineering task was accomplished by moving the gripper with a magnet to place it on top of the object (with dimensions as small as  $200\ \mu\text{m}$ ). The gripper closing was triggered by the addition of  $\text{CH}_3\text{COOH}$ . The gripper closed and securely held the object which could then be moved to a specified location. When the gripper was at this location,  $\text{H}_2\text{O}_2$  was added to the solution to cause the gripper to open and release its contents (Figure 3a–d). Experiments such as these were repeated several times with a range of objects including glass beads, wires, and tubes.

In conclusion, we have described reversible, chemo-mechanically triggered microgrippers that were used to pick and place objects. Such tools do not exist at the present time, and we anticipate their utility in laboratory-on-a-chip applications, reconfigurable microfluidic systems, and micromanufacturing.

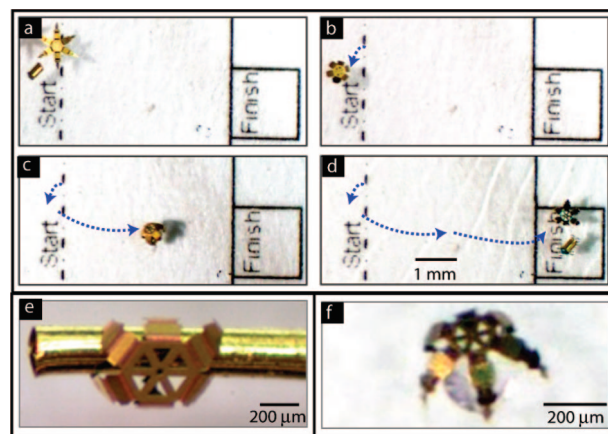


**Figure 3.** (a–d) Video microscopy snapshots showing pick-and-place of a  $200\ \mu\text{m}$  diameter gold tube. (e) Optical microscopy zoom image of microgripper holding on to a long  $200\ \mu\text{m}$  diameter gold tube. (f) Optical microscopy image showing a smaller microgripper holding onto a  $200\ \mu\text{m}$  diameter glass bead.

Here, the chemicals used to trigger our microgrippers are not compatible with living organisms; actuation under biological conditions for biopsy applications is explored elsewhere.<sup>10</sup> This communication represents a convincing proof-of-concept of an MCMS pick-and-place microgripper, and other material combinations of the trilayer hinges (such as the inclusion of lithographically patterned gels and smart polymers as triggers)<sup>11</sup> need to be explored to enable multiuse reversible operation and actuation with other chemicals.

**Acknowledgment.** This material was supported by the NSF under Grant Number CMMI-0448816 and DMR05-20491 and from the Dreyfus and the Beckman Foundations. We also acknowledge George Stern for theoretical modeling work.

**Supporting Information Available:** Details of fabrication methods, kinetics of microgripper closing with varying concentration of  $\text{CH}_3\text{COOH}$ , etch rates of Cu and Cr with  $\text{CH}_3\text{COOH}$  and  $\text{H}_2\text{O}_2$ , theoretical model details, and pick-and-place videos. This material is available free of charge via the Internet at <http://pubs.acs.org>.

## References

- (1) (a) Cecil, J.; Vasquez, D.; Powell, D. *Int. J. Prod. Res.* **2005**, *43*, 819–828. (b) Andersen, K. N.; Carlson, K.; Petersen, D. F.; Molhave, K.; Eichhorn, V.; Fatikow, S.; Boggild, P. *Microelectron. Eng.* **2008**, *85* (5–6), 1128–1130. (c) Buckley, P. R.; McKinley, G. H.; Wilson, T. S.; Small, W.; Bennett, W. J.; Bearinger, J. P.; McElfresh, M. W.; Maitland, D. J. *IEEE Trans. on Biomed. Eng.* **2006**, *53* (10), 2075–2083. (d) Shahinpoor, M.; Bar-Cohen, Y.; Simpson, J. O.; Smith, J. *Smart Mater. Struct.* **1998**, *7* (6), R15–R30. (e) Lu, Y. W.; Kim, C. J. *Appl. Phys. Lett.* **2006**, *89* (16), 164101–164103.
- (2) Kuby, J. *Immunology*; W. H. Freeman & Co: 1998.
- (3) Epstein, I. R.; Pojman, J. A. *An Introduction to Nonlinear Chemical Dynamics: Oscillations, Waves, Patterns, and Chaos*; Oxford University Press: 1998.
- (4) Leong, T. G.; Benson, B. R.; Call, E. K.; Gracias, D. H. *Small* **2008**, *4* (10), 1605–1609.
- (5) Prinz, V. Ya.; Seleznev, V. A.; Samoylov, V. A.; Gutakovskiy, A. K. *Microelectron. Eng.* **1996**, *30*, 439–442.
- (6) Chavez, K. L.; Hess, D. W. *J. Electrochem. Soc.* **2003**, *150* (4), G284–G291.
- (7) (a) Du, T.; Vijayakumar, A.; Desai, V. *Electrochim. Acta* **2004**, *49* (25), 4505–4512. (b) Chavez, K. L.; Hess, D. W. *J. Electrochem. Soc.* **2001**, *148* (11), G640–G643.
- (8) Nikishkov, G. P. *J. Appl. Phys.* **2003**, *94* (8), 5333–5336.
- (9) Lee, M. H.; Rowland, J. J. *Intelligent Assembly Systems*; World Scientific Publishing Co., Inc.: 1995.
- (10) Leong, T. G.; Randall, C. L.; Benson, B. R.; Bassik, N.; Stern, G. M.; Gracias, D. H. 2008. submitted.
- (11) (a) Guan, J. J.; He, H. Y.; Hansford, D. J.; Lee, L. J. *J. Phys. Chem. B* **2005**, *109* (49), 23134–23137. (b) Bassik, N.; Abebe, B.; Gracias, D. H. *Langmuir* **2008**, *24* (21), 12158–12163.

JA806961P

# Pick-and-Place using Chemically Actuated Microgrippers

Jatinder S. Randhawa<sup>†</sup>, Timothy G. Leong<sup>†</sup>, Noy Bassik<sup>†#</sup>, Bryan R. Benson<sup>†</sup>, Matthew T. Jochmans<sup>◊</sup>,

David H. Gracias<sup>†\*\*</sup>

<sup>†</sup>Department of Chemical and Biomolecular Engineering, Johns Hopkins University, Baltimore, MD 21218, <sup>#</sup>School of Medicine, Johns Hopkins University, Baltimore, MD 21205, <sup>◊</sup>Towson High School, Baltimore, MD 21286, <sup>\*</sup>Department of Chemistry, Johns Hopkins University, Baltimore MD 21218.

## Supplementary Information

### 1. Details of the fabrication of the microgrippers

A sacrificial layer of polyvinyl alcohol (PVA MW 6000, Polysciences) was spun on a Si wafer. A thin layer of chromium (Cr, 50 nm) was evaporated followed by copper (Cu, 250 nm).

#### **First step of photolithography**

1. Photopatternable polymer (Microposit<sup>TM</sup> SC 1827) was spincoated and baked for 1 min at 115 °C.
2. The first layer mask was used to expose the photoresist to UV and pattern the microgrippers. At this step all the phalanges were patterned.
3. Six  $\mu\text{m}$  thick nickel was electroplated to form the phalanges and 0.5  $\mu\text{m}$  of gold was electroplated as a protective coating on the nickel to enhance etch selectivity.

#### **Second step of photolithography**

1. Another layer of photopatternable polymer (Microposit<sup>TM</sup> SC 1827) was spincoated.
2. The mask for the hinges was exposed after alignment with the first layer. After developing in (Microposit<sup>TM</sup> 351 Developer), the photopatternable polymer was left behind as the hinges.

The underlying layer of Cu was etched in APS-100 (Technic, Inc.) and Cr was etched in CRE-473 (Technic, Inc.). The PVA was dissolved in water, releasing the grippers from the Si wafer.

### 2. Kinetics of microgripper closing with varying concentration of Acetic Acid ( $\text{CH}_3\text{COOH}$ )

In order to characterize the rate of closing as a function of  $\text{CH}_3\text{COOH}$  concentration, open

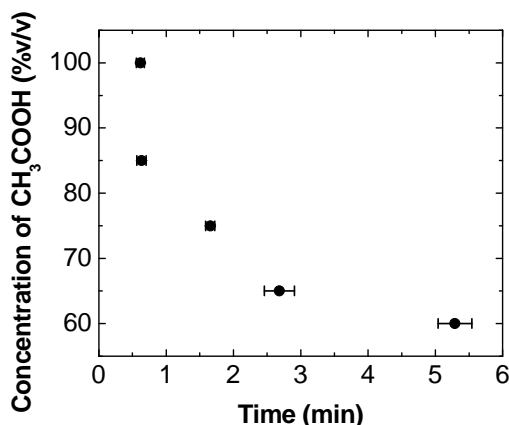


**Figure1:** A plot of the concentration of aqueous  $\text{CH}_3\text{COOH}$  solution and the time required for the grippers to close completely. The grippers close faster in higher concentrations of  $\text{CH}_3\text{COOH}$

grippers were placed into CH<sub>3</sub>COOH solutions of varying concentrations, and the time required for closing was recorded. We observed that the microgrippers closed faster in higher concentrations of CH<sub>3</sub>COOH (Fig. 1).

### **3. Etch rates of Cu and Cr with CH<sub>3</sub>COOH and H<sub>2</sub>O<sub>2</sub>**

Cu and Cr films of different thickness were evaporated onto transparent glass slides and these

<b>Concentration</b>	<b>Cu film</b>	<b>Cr film</b>
50% CH <sub>3</sub> COOH	No etching observed	No etching observed
100% CH <sub>3</sub> COOH	No etching observed	No etching observed
1% H <sub>2</sub> O <sub>2</sub>	No etching observed	No etching observed
30 % H <sub>2</sub> O <sub>2</sub>	No etching observed	No etching observed
50% CH <sub>3</sub> COOH + 1% H <sub>2</sub> O <sub>2</sub>	Etches completely [Etch Rate =1.12 ± 0.2 (nm/sec )]	No etching observed
75% CH <sub>3</sub> COOH + 5% H <sub>2</sub> O <sub>2</sub>	Etches completely [Etch Rate =3.5 ± 0.43 (nm/sec )]	No etching observed

**Table 1:** Etch rate of Cr and Cu in different concentrations of CH<sub>3</sub>COOH (v/v) and H<sub>2</sub>O<sub>2</sub> (w/w) at 20 °C. Each observation was noted after an hour and repeated three times.

Slides were immersed in different concentrations of CH<sub>3</sub>COOH and H<sub>2</sub>O<sub>2</sub>. Etch rates were measured by calculating the time for complete dissolution and assuming a uniform etch rate. It should be noted that complete etching of Cu was needed to reopen the gripper.

### **4. Theoretical Model Details**

#### **Background**

When metallic thin films are deposited in layers, they can exhibit stress due to several mechanisms: differences in thermal expansion, crystal lattice mismatch or other ‘intrinsic’ mechanisms, such as those associated with grain growth. In a Cr/Cu bilayer, the stressed Cr layer can relax upon release of the bilayer from the substrate by bending the bilayer (provided the two films do not delaminate).

#### **Multilayer thin film curvature model**

The expected bend angle from the layered hinge can be extracted by conducting a mechanical force balance across the strains of each layer. The multilayer stack will bend around a central location,  $y_b$ , where the bending moment is zero. Primary parameters include the Cr thin film stress, Young’s modulus and Poisson’s ratio of all layers. This model used to calculate joint curvature was adapted from literature.<sup>1</sup> The model was adapted for three layers; two layer simulations were performed by setting the thickness of the third layer to zero.

Definitions used in the model:

$E$  : Young's (elastic) modulus,  $\nu$  : Poisson's ratio,  $t$  : thickness,  $\sigma^0$  : initial stress,  $\varepsilon^0$  : initial strain,  $R$  : radius of curvature,  $y$  : vertical position relative to substrate,  $y_b$  : location where bending moment = 0,  $\eta$  : a parameter

**The assumptions in this model are:**

- A) The layers are made of an elastically isotropic material
- B) Strain normal to the surface is zero ( plane strain conditions )
- C) Cr layer: Initial stress within the Cr layer is uniform  
 $E = 144 \text{ GPa}$ ,  $\nu = 0.21$ ,  $t = 50 \text{ nm}$
- D) Cu layer: Zero stress  
 $E = 130 \text{ GPa}$ ,  $\nu = 0.34$ ,  $t = 250 \text{ nm}$
- E) Polymer layer: Zero stress  
 $E = 1 \text{ GPa}$  [note H],  $\nu = 0.3$ ,  $t = 3500 \text{ nm}$
- E) Stress in the Cr layer was measured via wafer bending to be 1.017 GPa
- F) Constant temperature conditions
- G) Polymer and Cu are etched in a linear fashion from the surface down (isotropic etch).
- H) The elastic moduli of polymers varies greatly as a function of processing conditions. We modeled the initial hinge using a typical elastic modulus reported in literature. This value affects only the rate at which the hinge opens and closes, changing its open state minimally.

**Equations used in the model, general parameters for multiple layers:**

$$c = \frac{\sum_{i=1}^n E'_i t_i \eta_i \varepsilon_i^0}{\sum_{i=1}^n E'_i t_i} \quad y_b = \frac{\sum_{i=1}^n E'_i t_i (y_i + y_{i-1})}{\sum_{i=1}^n E'_i t_i} \quad y_i = y_{i-1} + t_i; y_0 = 0$$

$$E'_i = \frac{E_i}{1 - \nu_i^2}, \eta_i = 1 + \nu_i, \varepsilon_i^0 = \frac{\sigma_i^0}{E_i} \quad R = \frac{2 \sum_{i=1}^n E'_i t_i [y_i^2 + y_i y_{i-1} + y_{i-1}^2 - 3y_b (y_i + y_{i-1} - y_b)]}{3 \sum_{i=1}^n E'_i t_i (y_i + y_{i-1} - 2y_b) (c - \eta_i \varepsilon_i^0)}$$

**Modeling to explain experimental observations**

In order to model the reactions encountered in the gripper, equilibrium folding angles were calculated for a variety of thicknesses. The simulation began with parameters equivalent to those used to fabricate the gripper with Cr, Cu, and polymer layers (Figure 1A in the manuscript). As the polymer layer was removed, its thickness decreased while other properties remained the same, the model was solved for all relevant polymer layer thickness - this generated the graph in Figure 2 c-d (in the manuscript). At this point, the model considered two layers: Cr and Cu. Mechanical equilibrium folding indicated a closed gripper with an angle of approximately 68°, this corresponded with observations. The model was now solved for successively decreasing values of the Cu layer, corresponding to Cu removal. The hinge angle now increased in the model (peaking at approximately 400°). When all Cu was removed, the model was solved for a relaxed, bare Cr sheet, which has a 0° hinge angle.

## **References**

- (1) G. P. Nikishkov, *J. Appl. Phys.* **2003**, *94*, 5333.
- (2) Z. Q. Qi, E. I. Meletis, *Thin Solid Films* **2005**, *479*, 174.
- (3) L. B. Freund, S. Suresh, *Thin film materials : stress, defect formation, and surface evolution*, Cambridge University Press, Cambridge, UK ; New York **2003**.
- (4) Y. K. Hong, R. R. A. Syms, *Sensor. Actuat. A-Phys.* **2006**, *127*, 381.